Evolution of the mass-transfer processes in nonideal dissipative systems. I. Numerical simulation

O. S. Vaulina, X. G. Adamovich, O. F. Petrov, and V. E. Fortov
Joint Institute for High Temperatures, RAS 125412, Izhorskaya Street, 13/19, Moscow, Russia
(Received 28 December 2007; published 10 June 2008)

The results of numerical study of mass-transfer processes in quasi-two- and three-dimensional nonideal dissipative systems are presented. Simulations were performed for different types of model pair potentials of intergrain interaction that are various combinations of power-law and exponential functions. The calculations were performed in a wide range of parameters typical for laboratory dusty plasma experiments. It was shown that the dynamics of grains in liquidlike systems for short observation times is close to the evolution of thermal oscillations in the crystal lattice.

DOI: 10.1103/PhysRevE.77.066403 PACS number(s): 52.27.Lw, 52.65.Yy, 82.70.Dd

I. INTRODUCTION

The problems associated with mass-transfer processes in dissipative systems of interacting particles are of great interest in various fields of science (plasma physics, the medical industry, physics and chemistry of polymers, etc.) [1–9]. Nevertheless, hydrodynamic approaches can successfully describe these processes only in the case of short-range interactions between particles. The main problem involved in studies of nonideal systems is associated with the absence of an analytical theory of liquids. To predict the transport properties of nonideal systems, various empirical approaches and computer simulations of the dynamics of the particles with different models for the potentials of their interaction are used [1–5]. The simulations of transport processes are commonly performed by methods of molecular dynamics, which are based on solution of reversible equations of motion of the particles, or Langevin equations taking into account the irreversibility of the processes under study.

Diffusion is the basic mass-transfer process, defining the losses of energy (dissipation) in a system of particles and its dynamic features (such as the phase state, the conditions of propagation of waves, and the formation of instabilities). When the deviations of the system from statistical equilibrium are small, the kinetic coefficients of linear dissipative processes (constants of diffusion, viscosity, thermal conductivity, etc.) can be found from Green-Kubo formulas that were established with the help of the theory of Markovian stochastic processes under the assumption of a linear reaction of the statistical system to small perturbations. These formulas are important results of the statistical theory of irreversible processes. According to these formulas, the diffusion coefficient D can be found from the following relationship:

$$D = \int_0^\infty \langle V(0)V(t)\rangle dt/m. \tag{1}$$

Here $\langle V(0)V(t)\rangle$ is the velocity autocorrelation function (VAF) of grains, t is the time, and m is the dimension of the system. The diffusion coefficient can also be obtained from the analysis of thermal transfer of the grains through unit area of the medium:

$$D = \lim_{t\to\infty}\langle(\Delta l)^2\rangle/(2mt), \tag{2}$$

where $\Delta l = \Delta l(t)$ is the displacement of an isolated particle from its initial position during the time t. In both Eqs. (1) and (2), the brackets $\langle\ \rangle$ denote ensemble and time averaging (averaging for all time intervals with duration t). As the relationships (1) and (2) were obtained without any assumptions on the nature of thermal motion, they are valid for gases as well as for liquids and solids in the case of small deviations of the system from its steady state condition. In the general case of nonideal fluids, analytical solutions of Eqs. (1) and (2) are unavailable, which makes it impossible to find the diffusion coefficient. The simple solution $D \equiv D_0 = T/(\nu_{\rm fr} M)$, known as the Einstein relationship, exists only for noninteracting ("Brownian") particles; here M and T are the mass and the temperature of a grain, respectively, and $\nu_{\rm fr}$ is the friction coefficient.

Due to the existing level of experimental physics, it is necessary to go beyond the bounds of the diffusion approximation, and modern methods of numerical simulation (based on the theory of stochastic processes) allow one to do this. A description within macroscopic kinetics may be insufficient for the analysis of mass-transfer processes on physically small time intervals. A study of the mass-transfer processes for short observation times is especially important for investigation of fast processes (e.g., the propagation of shock waves and impulse actions, or progression of the front of a chemical transformation in condensed matter [5,6]), and also for the analysis of transport properties of strongly dissipative media (such as colloidal solutions, plasmas of combustion products, nuclear-induced high-pressure dusty plasmas [2,8,9]), where long-term experiments should be carried out to measure the diffusion coefficients correctly.

II. MASS-TRANSFER PROCESSES IN NONIDEAL MEDIA

Consider the particle motion in a homogeneous dissipative medium. One can find the displacement of the jth particle in this medium along one coordinate, $x_j = x_j(t)$, under the action of some potential F and random forces $F_{\rm ran}$ from the Langevin equation

$$M\frac{d^2x_j}{dt^2} = -M\nu_{\rm fr}\frac{dx_j}{dt} + F + F_{\rm ran}. \tag{3}$$

In a statistical equilibrium of a system of particles $[M\langle(dx_j/dt)^2\rangle = \langle MV_x(t)^2\rangle \equiv T]$ the mean value of the random

force is zero, $\langle F_{\rm ran}(t)\rangle=0$, and its autocorrelation function $\langle F_{\rm ran}(0)F_{\rm ran}(t)\rangle=2B\delta(t)$ corresponds to the δ-correlated Gaussian process, where $\delta(t)$ is the delta function, and $B=T\nu_{\rm fr}M$ (due to the fluctuation-dissipation theorem). Under these assumptions Eq. (1) describes a Markovian stochastic process.

To analyze the dependence of mass transfer on time t, we introduce the following functions:

$$D_{\rm GK}(t)=\int_0^t\langle V_x(0)V_x(t)\rangle dt, \tag{4a}$$

$$D_{\rm MSD}(t)=\langle (x_j)^2\rangle/(2t), \tag{4b}$$

where $V_x(t)=dx_j/dt$ is the velocity of the jth particle. The function $D_{\rm GK}(t)$ (4a) is defined using the well-known Green-Kubo (GK) formulas, and the function $D_{\rm MSD}(t)$ (4b) uses the information about the mean-square displacement (MSD) of particles. With small deviations of the system from the equilibrium state, both functions $[D_{\rm GK}(t)$ and $D_{\rm MSD}(t)]$ as $t\to\infty$ should tend to the same constant $D=\lim_{t\to\infty}D(t)$, which corresponds to the standard definition of the diffusion coefficient.

Neglecting the interparticle interaction ($F=0$, the case of Brownian particles), one can find the VAF, using the formal solution of Eq. (3) under the assumption $\langle F_{\rm ran}(t)V_x(0)\rangle=0$ [2]:

$$\langle V_x(0)V_x(t)\rangle=\frac{T}{M}\exp(-\nu_{\rm fr}t). \tag{5}$$

Then the mass-transfer evolution function $D_{\rm GK}(t)$, Eq. (4a), may be written as

$$D_{\rm GK}(t)=D_0[1-\exp(-\nu_{\rm fr}t)]. \tag{6a}$$

To find the mean-square displacement of the jth particle, one should multiply Eq. (3) by x_j. Then, if there is no correlation between the slow particle motion and the "fast" stochastic impact ($\langle F_{\rm ran}x_j\rangle=0$), the simultaneous solution of Eqs. (3) and (4b) in a homogeneous medium $[M\langle(dx_j/dt)^2\rangle\equiv T,\ \langle(\Delta l)^2\rangle=m\langle x_j^2\rangle]$ can be presented as [5]

$$D_{\rm MSD}(t)/D_0=1-[1-\exp(-\nu_{\rm fr}t)]/\nu_{\rm fr}t. \tag{6b}$$

Thus, for the Brownian case, when $t\to\infty$ and $\nu_{\rm fr}t\gg 1$, we have $D_{\rm GK}(t)=D_{\rm MSD}(t)\to D_0$, and on small time intervals ($\nu_{\rm fr}t\ll 1$) the motion of particles has a ballistic character: $\langle x^2\rangle\equiv\langle x_j^2\rangle\approx Tt^2/M$ and $D_{\rm MSD}(t)=\langle x^2\rangle/(2t)\propto t$.

The analytical solution of Eq. (3) may also be obtained for an ideal crystal under the assumption that the restoring force $F=-M\omega_c^2x_j$ acting on particles in lattice sites can be described by the single characteristic frequency ω_c (the case of a harmonic oscillator). In this case we will have

$$M\frac{d^2x_j}{dt^2}=-M\nu_{\rm fr}\frac{dx_j}{dt}-M\omega_c^2x_j+F_{\rm ran}. \tag{7}$$

After multiplying both parts of this equation by $x=x_j$, rearranging, and averaging, taking into account that $\langle F_{\rm ran}x\rangle=0$ and $M\langle(dx/dt)^2\rangle=M\langle V_x(t)^2\rangle\equiv T$, we will obtain [10]

$$M\frac{d^2\langle x^2\rangle}{dt^2}=-M\nu_{\rm fr}\frac{d\langle x^2\rangle}{dt}-2M\omega_c^2\langle x^2\rangle+2T. \tag{8}$$

Then the simultaneous solution of Eqs. (8) and (4b) can be written as

$$\frac{D_{\rm MSD}(t)}{D_0}=\frac{1-\exp(-\nu_{\rm fr}t/2)[\cosh(\nu_{\rm fr}t\psi)+\sinh(\nu_{\rm fr}t\psi)/\{2\psi\}]}{2\xi_c^2\nu_{\rm fr}t}, \tag{9}$$

where $\psi=(1-8\xi_c^2)^{1/2}/2$, and $\xi_c=\omega_c/\nu_{\rm fr}$. In the case of $(1-8\xi_c^2)<0$, the ψ value is imaginary: $\psi=i\psi^*$, where $\psi^*=(8\xi_c^2-1)^{1/2}/2$. In this case, $\sinh(i\psi^*\nu_{\rm fr}t)=i\sin(\psi^*\nu_{\rm fr}t)$, $\cosh(i\psi^*\nu_{\rm fr}t)=\cos(\psi^*\nu_{\rm fr}t)$, and the expression for $D_{\rm MSD}(t)$ function will include the trigonometric functions instead of the hyperbolic functions.

To define the VAF $\langle V_x(0)V_x(t)\rangle\equiv\langle V_x(t_0)V_x(t_0+\tau)\rangle$, we will use the following designations: $V_x(t_0)\equiv V_0$, $V_x(t_0+\tau)\equiv V$, $X(t_0)=x$, $X(t_0+\tau)\equiv x+\Delta x$. Equation (7) can be presented as two expressions at two different instants of time ($t=t_0$ and $t=t_0+\tau$). Then we can multiply the first of them by V and the second by V_0. The sum of these two expressions, averaged over the particle ensemble for all time intervals with the duration $t=\tau$ [taking into account that $\langle x\Delta x\rangle=0$, $\langle F_{\rm ran}(t_0)V(t_0+\tau)\rangle=\nu_{\rm fr}M\langle V(t_0)V(t_0+\tau)\rangle$, and $\langle F_{\rm ran}(t_0+\tau)V(t_0)\rangle=0$ [2,5]], can be written as

$$\frac{d\langle V_0V\rangle}{dt}=-\nu_{\rm fr}\langle V_0V\rangle-\omega_c^2\frac{d\langle x^2\rangle}{dt}. \tag{10}$$

The solution of this equation is

$$\langle V_0V\rangle=\frac{1}{2}\frac{d^2\langle x^2\rangle}{dt^2}, \tag{11}$$

and Eq. (10) may be rewritten as

$$\frac{d^2\langle V_0V\rangle}{dt^2}=-\nu_{\rm fr}\frac{d\langle V_0V\rangle}{dt}-2\omega_c^2\langle V_0V\rangle. \tag{12}$$

Thus, in this case of a harmonic oscillator, we will have for the VAF

$$\langle V_x(0)V_x(t)\rangle=\frac{T}{M}\exp(-\nu_{\rm fr}t/2)[\cosh(\nu_{\rm fr}t\psi)-\sinh(\nu_{\rm fr}t\psi)/\{2\psi\}], \tag{13}$$

and the simultaneous solution of Eqs. (13) and (4a) can be written as

$$\frac{D_{\rm GK}(t)}{D_0}=\frac{\exp(-\nu_{\rm fr}t/2)}{\psi}\sinh(\nu_{\rm fr}t\psi). \tag{14}$$

When ψ is imaginary, both expressions for the VAF and $D_{\rm MSD}(t)$ functions [Eqs. (13) and (14)] will include the trigonometric functions instead of the hyperbolic ones (see above).

The normalized VAF $f(t)=M\langle V_x(0)V_x(t)\rangle/T$ and mass-transfer evolution functions $[D_{\rm GK}(t)/D_0,\ D_{\rm MSD}(t)/D_0]$ for various values of ξ_c are presented in Fig. 1, where the time is given in units of the inverse friction coefficient ($\nu_{\rm fr}^{-1}$). It is easy to see that for short observation times a particle in a

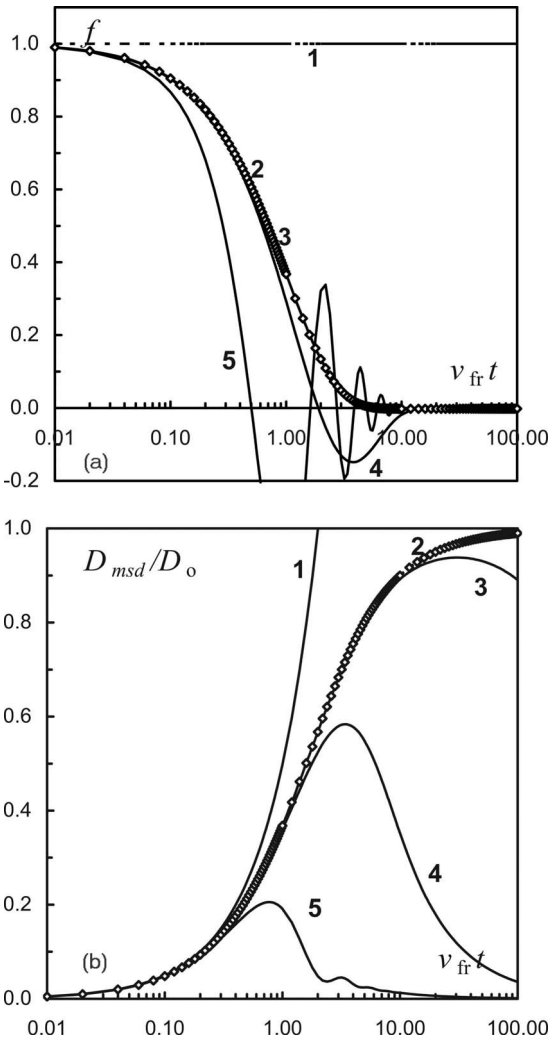

FIG. 1. Functions $f(t\nu_{\rm fr})$ (a) and $D_{\rm MSD}(t\nu_{\rm fr})/D_0$ (b) for (1) ballistic mode [$f(t)=1$, $D_{\rm MSD}(t)\propto t$]; (2) Brownian case [Eqs. (5) and (6b)]; and for the harmonic oscillator [Eqs. (13) and (9)] with different ξ_c: (3) 0.033, (4) 0.38, and (5) 2.

lattice site also has a ballistic character of motion [$\langle x^2\rangle \approx Tt^2/M$, $D_{\rm MSD}(t)=\langle x^2\rangle/(2t)\propto t$]. With increasing time ($\nu_{\rm fr}t\gg 1$) both evolution functions tend to zero, $D_{\rm GK}(t)=D_{\rm MSD}(t)\to 0$, because for the harmonic oscillator the mean-square displacement $\langle(\Delta l)^2\rangle$ is constant: $\langle(\Delta l)^2\rangle=mT/(M\omega_c^2)$.

For liquid media, an exact analytic expression for $\langle V_x(0)V_x(t)\rangle$, $D_{\rm GK}(t)$, and $D_{\rm MSD}(t)$ cannot be obtained. Nevertheless, we should note some features of the relations between the mentioned functions, both in the case of Brownian particles [see Eqs. (5) and (6b)] and in the case of the harmonic oscillator [see Eq. (13)], and which may occur for liquids:

$$D_{\rm GK}(t)\frac{d\{tD_{\rm MSD}(t)\}}{dt}\equiv\frac{1}{2}\frac{d\langle x^2\rangle}{dt}, \tag{15a}$$

$$\langle V_x(0)V_x(t)\rangle=\frac{d^2\{tD_{\rm MSD}(t)\}}{dt^2}\equiv\frac{1}{2}\frac{d^2\langle x^2\rangle}{dt^2}. \tag{15b}$$

The mean-square displacement evolution $D_{\rm MSD}(t)$ was studied numerically in [10–12] for nonideal systems with a screened Coulomb pair interaction potential (of Yukawa type):

$$U=(eZ)^2\exp(-r/\lambda)/r. \tag{16}$$

Here r is the distance between two particles with a charge eZ, where e is the electron charge, λ is the screening length, $\kappa=l_p/\lambda$, and l_p is the mean interparticle distance, which is equal to the inverse square root from the surface density of particles for two-dimensional (2D) systems, and it is the inverse cubic root of their bulk concentration in three-dimensional case. As a result of numerical simulation, the characteristic frequencies for the body-centered cubic (bcc) lattice, $\omega_c=\omega_{\rm bcc}\approx 2eZ\exp(-\kappa/2)[(1+\kappa+\kappa^2/2)/(l_p^3M\pi)]^{1/2}$, and for the hexagonal lattice, $\omega_c=\omega_h\approx 1.16\omega_{\rm bcc}$, were obtained [10–12]. It was also shown that these frequencies are responsible for the mean time t_a of "settled life" of particles in liquidlike systems and their values define the evolution of mass transfer for observation times $t<t_a\approx 2/\omega_c$. Taking into account Eqs. (15a) and (15b), it is easy to assume that the behavior of the VAF and $D_{\rm GK}(t)$ for the mentioned observation times in liquidlike Yukawa systems is also close to the behavior of these functions for harmonic oscillator.

The dynamics of 3D systems of particles with various types of pair isotropic potentials was numerically investigated in [13]. Those potentials represented different combinations of power-law and exponential functions, commonly used for simulations of repulsion in the kinetics of interacting particles [5]:

$$U=U_c[b_1\exp(-\kappa_1 r/l_p)+b_2(l_p/r)^n\exp(-\kappa_2 r/l_p)]. \tag{17}$$

Here $b_{1(2)}$, $\kappa_{1(2)}=l_p/\lambda_{1(2)}$, and n are variable parameters, and $U_c=(eZ)^2/r$ is the Coulomb potential. In the context of investigation of dusty plasma properties the screened Coulomb potential (16) ($b_1=1$, $b_2=0$, $\kappa_1=l_p/\lambda$) is of particular interest. But it should be noted that the simple model (16) agrees with numerical and experimental results in a complex plasma only for short distances $r<\lambda$ between two isolated macroparticles in a plasma [14–17]. With increasing distance, the effect of the screening weakens, and the asymptotic character of the potential U for large distances $r\gg\lambda$ can follow a power-law dependence, $U\propto r^{-2}$ [16] or $U\propto r^{-3}$ [17]; thus, the parameters of the potentials (17) will be $\kappa_1=l_p/\lambda$, $\kappa_2=0$, $n=1,2$, and $b_1\gg b_2$, respectively.

It was noticed that the mass-transfer processes and spatial correlation of macroparticles in these 3D systems are defined by the ratio of the second derivative U'' of the pair potential $U(r)$ at the point of the mean interparticle distance $r=l_p$ to the grain temperature T, if the following empirical condition is met [13]:

$$2\pi>|U'(l_p)|l_p/|U(l_p)|>1. \tag{18}$$

In this case, the spatial correlation of particles did not depend on the friction ($\nu_{\rm fr}$) and was defined by the value of effective coupling parameter $\Gamma^*=Ml_p^2U''/(2T)$ in the range between $\Gamma^*\sim 10$ and the point of crystallization of the system ($\Gamma^*\sim 100$), where for all considered cases formation of the bcc structure was observed with the characteristic oscillation frequency of the grains [13]:

$$\omega_c^2 = \omega_{\mathrm{bcc}}^2 \equiv 2|U''(l_p)|/(\pi M). \tag{19a}$$

It is natural to expect that the characteristic oscillation frequency in the hexagonal lattice for the grains, interacting with the potentials (17), may be written similarly to the frequency found for quasi-2D Yukawa systems [10,11]:

$$\omega_c^2 = \omega_h^2 \equiv 2.7|U''(l_p)|/(\pi M). \tag{19b}$$

The behavior of the VAFs and of the evolution functions $D_{\mathrm{MSD}}(t)$, $D_{\mathrm{GK}}(t)$ is studied numerically in the next part of this paper for quasi-2D and 3D nonideal systems with different interaction potentials, which obey Eqs. (17) and (18).

III. PARAMETERS OF NUMERICAL SIMULATION

The simulation was carried out by the Langevin molecular dynamics method based on the solution of a system of differential equations with the stochastic force F_{ran}, which takes into account processes leading to the established equilibrium (stationary) temperature T of macroparticles that characterizes the kinetic energy of their random (thermal) motion. The simulation technique is detailed in Refs. [10–12,18]. The considered system of N_p motion equations (N_p is the number of grains) included also the forces of pair interparticle interaction $\boldsymbol{F}_{\mathrm{int}}$ and external forces $\boldsymbol{F}_{\mathrm{ext}}$:

$$M\frac{d^2\vec{l}_k}{dt^2} = \sum_j F_{\mathrm{int}}(l)|_{l=|\vec{l}_k-\vec{l}_j|}\frac{\vec{l}_k-\vec{l}_j}{|\vec{l}_k-\vec{l}_j|} + \vec{F}_{\mathrm{ext}} - M\nu_{\mathrm{fr}}\frac{d\vec{l}_k}{dt} + \vec{F}_{\mathrm{ran}}. \tag{20}$$

Here $F_{\mathrm{int}}(l) = -\partial U/\partial l$, and $l = |\vec{l}_k - \vec{l}_j|$ is the interparticle distance. To analyze the equilibrium characteristics in systems of particles interacting with potentials (17), the motion equations (20) were solved with various values of the effective parameters that are responsible for the mass transfer and phase states in dissipative nonideal systems. These parameters were introduced by analogy with the parameters found in [11–13], namely, the effective coupling parameter

$$\Gamma^* = a_1 l_p^2 U''(l_p)/(2T) \tag{21}$$

and the scaling parameter

$$\xi = \omega^*/\nu_{\mathrm{fr}} \quad \text{where} \quad \omega^* = |a_2 U''(l_p)|^{1/2}(2\pi M)^{-1/2}. \tag{22}$$

Here $a_1 = a_2 \equiv 1$ for 3D systems, and $a_1 = 1.5$, $a_2 = 2$ for the quasi-2D case. The calculations were carried out for a uniform 3D system and for a quasi-2D system simulating an extensive dusty layer. The scaling parameter was varied from $\xi \approx 0.04$ to $\xi \approx 3.6$ in the range typical for laboratory dusty plasmas in gas discharges; thus, the values of Z were varied from 500 to 50 000, the particle mass M was $10^{-11}-10^{-8}$ g, and the l_p values were $\sim 100-1000$ μm. The Γ^* value was varied from 10 to 120.

In the 3D case the external forces were absent ($|\boldsymbol{F}_{\mathrm{ext}}| \equiv 0$), and periodic boundary conditions were used for all three directions $\boldsymbol{x}$, $\boldsymbol{y}$, and $\boldsymbol{z}$. Most of the calculations were performed for 125 independent particles in a central calculation cell that was a cube with the characteristic size L. The length of the cell L (and the corresponding number of particles) was chosen in accordance with the condition of a correct simulation of the system's dynamics, $L \gg l_p|U(l_p)|/\{|U'(l_p)|l_p - |U(l_p)|\}$, which satisfies the requirement of strong reduction of the pair potential at the characteristic distance L [18]. So, for example, for the Yukawa potential this conditions may be presented in the form $l_p/L \ll \kappa$ [19]. The potential of the interparticle interaction was cut off at the distance $L_{\mathrm{cut}} \sim 4l_p$, which was defined from the condition of a weak disturbance of electrical neutrality of the system: $U'(L_{\mathrm{cut}})L_{\mathrm{cut}}^2 \ll (eZ)^2$. To prove that the results of the calculation are independent of the number of particles and the cutoff distance L_{cut}, additional test calculations were carried out for 512 independent particles with $L_{\mathrm{cut}} = 7l_p$ and $\Gamma^* = 1.5$, 17.5, 25, 49, and 92. The disagreement between the results of these calculations was within the limits of the numerical error and did not exceed $\pm(1-3)\%$.

In the quasi-2D case, the simulation was carried out for a monolayer of grains with periodic boundary conditions in the directions $\boldsymbol{x}$ and $\boldsymbol{y}$. In the $\boldsymbol{z}$ direction the gravitational force Mg, compensated by the linear electrical field $E_z = \beta z$ ($|\boldsymbol{F}_{\mathrm{ext}}| \equiv F_{\mathrm{ext}}^z = Mg - eZ\beta z$), was considered. Here β is the gradient of the electrical field, and $F_{\mathrm{ext}}^x = F_{\mathrm{ext}}^y \equiv 0$. The number of independent particles in the central calculated cell was varied from 256 to 1024; accordingly, the cutoff distance of the potential was changed from $5l_p$ to $25l_p$. The value of the gradient β of the electrical field E_z, confining the layer in the z direction, was varied from $\sim 10^{-2}$ to ~ 100 V/cm^2, and for the simulated monolayers of grains the β value was in agreement with the criterion of formation of monolayer dust structures proposed in [20]: $eZ\beta < 2\Sigma_{i=1}^{N_p} U'(l_i)/l_i$. Under this condition we have not detected any considerable dependence of the particle dynamics on the values of β and N_p in our simulations.

IV. RESULTS OF THE NUMERICAL SIMULATION AND THEIR DISCUSSION

The evolution of mass-transfer processes, obtained in the numerical experiments for quasi-2D and 3D systems with various interaction potentials for different values of ξ and Γ^* is illustrated in Figs. 2–5, where the normalized VAFs $f(\nu_{\mathrm{fr}}t) = M\langle V(0)V(\nu_{\mathrm{fr}}t)\rangle/(mT)$ and mass-transfer evolution functions $D_{\mathrm{GK}}(\nu_{\mathrm{fr}}t)/D_0$ and $D_{\mathrm{MSD}}(\nu_{\mathrm{fr}}t)/D_0$ are presented. In Figs. 2 and 3, the curves 1 are the solutions of the Langevin equation neglecting the interparticle interaction [see Eqs. (5), (6a), and (6b)]. It can be easily seen that, in the presence of interparticle interactions, the behavior of $\langle V(0)V(t)\rangle$, $D_{\mathrm{GK}}(t)$, and $D_{\mathrm{MSD}}(t)$ on short observation times ($\nu_{\mathrm{fr}}t \ll 1$) corresponds to the motion typical for Brownian particles. With time, the functions $D_{\mathrm{MSD}}(t)$ and $D_{\mathrm{GK}}(t)$ reach their maxima $D_{\mathrm{MSD}}^{\max}$ and $D_{\mathrm{GK}}^{\max}$. However, neither the relative magnitude $D_{\mathrm{MSD}}^{\max}/D_0$, $D_{\mathrm{GK}}^{\max}/D_0$ nor the position $t_{\max}\nu_{\mathrm{fr}}$ of these maxima depends on Γ^*; but they are defined by the value of the scaling parameter ξ for either the 3D problem or the simulated 2D system. This feature was noticed earlier for the functions $D_{\mathrm{MSD}}(t)$ [10–13].

It is easy to see that the evolution of the functions $\langle V(0)V(t)\rangle$, $D_{\mathrm{MSD}}(t)$, and $D_{\mathrm{GK}}(t)$ for systems with different pair potentials is defined by the particle temperature T, the

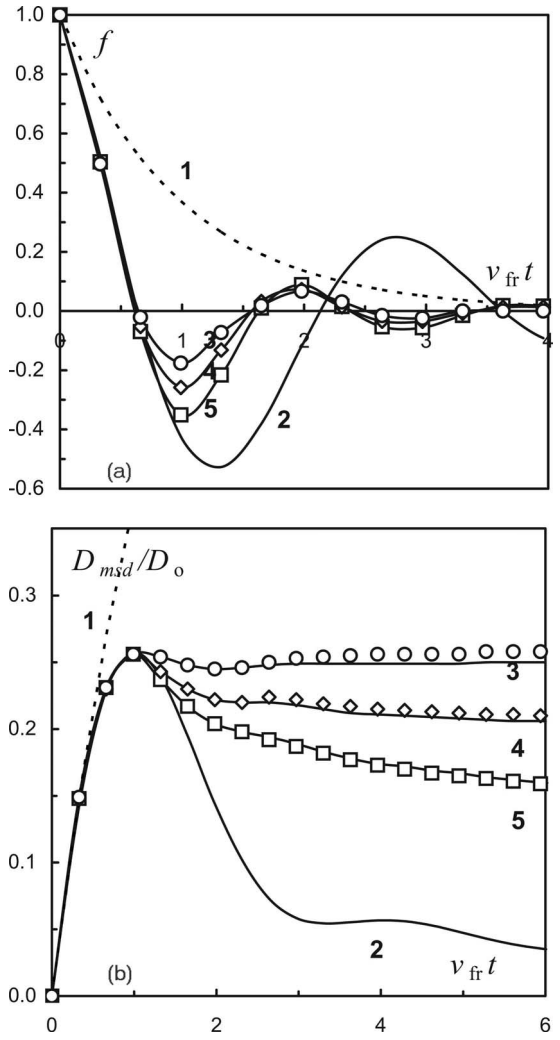

FIG. 2. Functions $f(t\nu_{fr})$ (a) and $D_{MSD}(t\nu_{fr})/D_0$ (b) for (1) Brownian case; (2) harmonic oscillator with $\xi_c=1.53$. Numerical results are also shown for quasi-2D problem with $\xi=0.93$ ($\xi_c=1.53$) and various Γ^*: (3) 12, (4) 27, and (5) 56; and for different potentials U: solid lines $U/U_c=\exp(-4r/l_p)$, circles $U/U_c=0.1\exp(-2r/l_p)+\exp(-4r/l_p)$, diamonds $U/U_c=\exp(-4r/l_p)+0.05l_p/r$, and squares $U/U_c=0.05(l_p/r)^3$.

effective coupling parameter Γ^*, and the scaling parameter ξ (see Figs. 2–5) and also that the relation between $D_{MSD}(t)$ and $D_{GK}(t)$ is in accordance with Eq. (15a) (see Fig. 3).

With $t\to\infty$, both the functions $D_{MSD}(t)$ and $D_{GK}(t)$ tend to the same constant value D which corresponds to the diffusion coefficient. The normalized coefficients $D^*=D(\nu_{fr}+\omega^*)M/T$ vs the Γ^* parameter for quasi-2D systems with various pair potentials are shown in Fig. 6. It can be easily noticed that the D^* value for the systems under study is defined by the value of Γ^*. It was observed that the difference between the diffusion coefficients of weakly dissipative ($\xi>0.3$) and weakly dispersive ($\xi<0.25$) quasi-2D structures with Γ^* between ~6 and ~97 is rather small; within the mentioned range of Γ^* the deviations of the diffusion coefficients from their mean value do not exceed 7%. This difference increases noticeably with an increase of $\Gamma^*>100$. These deviations were observed for quasi-2D Yukawa systems as well as for 3D systems with different types of pair potential [10–13]. Note that the obtained functions $D^*(\Gamma^*)$ have two critical points, one of which is a point of inflection ($\Gamma^*\sim 98-108$) that, possibly, reflects a phase transition between the hexatic phase and the liquid. The second critical point (the point of abrupt change of D) lies near $\Gamma^*\sim 153-165$, where $D\to 0$, and the system under study is transforming into a solid with a perfect hexagonal lattice. Similar behavior of $D^*(\Gamma^*)$ was observed for quasi-2D Yukawa systems [11]. The mean value of the normalized diffusion coefficient D^* averaged for different values of Z, κ, ν_{fr}, and β for quasi-2D systems with the different potentials is presented in Fig. 7, where the dependence $D^*(\Gamma^*)$ for 3D structures [12,13] is also shown.

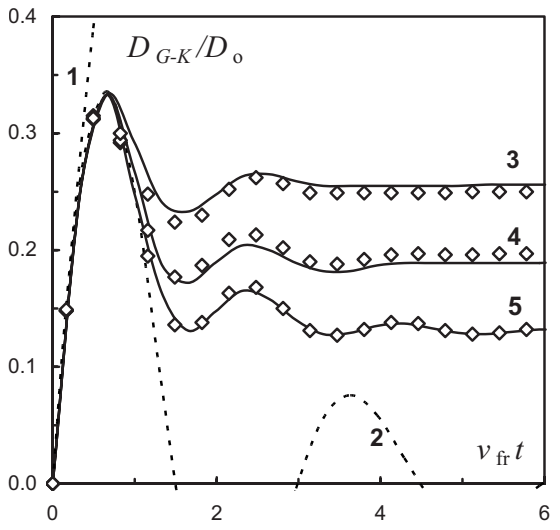

FIG. 3. Functions $D_{GK}(t\nu_{fr})/D_0$ for (1) Brownian case; (2) harmonic oscillator with $\xi_c=1.53$. Numerical results are also shown for quasi-2D problem ($\xi=0.93$, $\xi_c=1.53$) with different Γ^*: (3) 12, (4) 27, and (5) 56. Fine lines D_{GK}/D_0 from Eq. (4a); diamonds D_{GK}/D_0 from Eq. (15a).

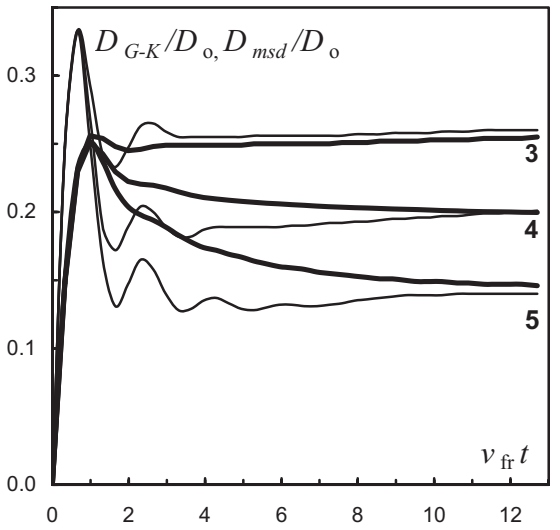

FIG. 4. Functions $D_{GK}(t\nu_{fr})/D_0$ [fine lines, Eq. (4a)] and $D_{MSD}(t\nu_{fr})/D_0$ [thick lines, Eq. (4b)] for quasi-2D problem ($\xi=0.93$, $\xi_c=1.53$) with different Γ^*: (3) 12, (4) 27 and (5) 56.

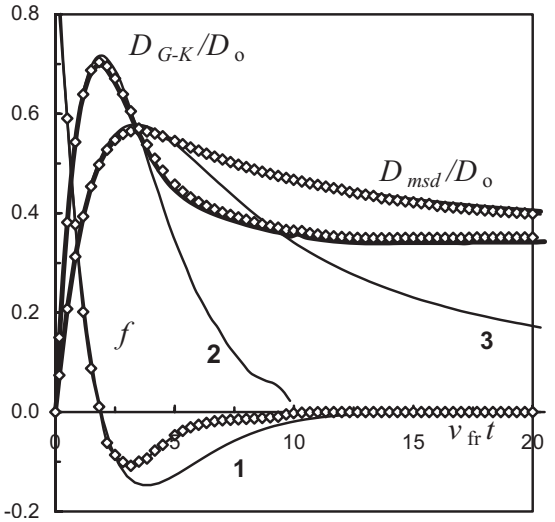

FIG. 5. Functions $f(t\nu_{fr})$ (1), $D_{GK}(t\nu_{fr})/D_0$ (2), and $D_{MSD}(t\nu_{fr})/D_0$ (3) for harmonic oscillator (fine lines) with ξ_c =0.19. Numerical results are also shown for 3D problem with .ξ =0.19 (ξ_c=0.38) and Γ^*=27 for different potentials U: thick lines $U/U_c=\exp(-2.4r/l_p)$; diamonds $U/U_c=\exp(-4.8r/l_p)+0.05l_p/r$.

The temperature dependence of the diffusion coefficient D of macroparticles in 3D systems with various types of potential and for quasi-2D structures with a screened Coulomb potential was found in [11–13]. There it was shown that the diffusion coefficient for strongly coupled liquidlike systems can be presented as

$$D \approx \frac{T\Gamma^*}{12\pi(\xi+1)\nu_{fr}M}\exp\left(-3\frac{\Gamma^*}{\Gamma_c^*}\right), \tag{23}$$

where Γ_c^* is the crystallization point of the structure under study (Γ_c^*=102 for the 3D problem and 98 for the 2D case). The approximation by Eq. (23) of the numerical results for

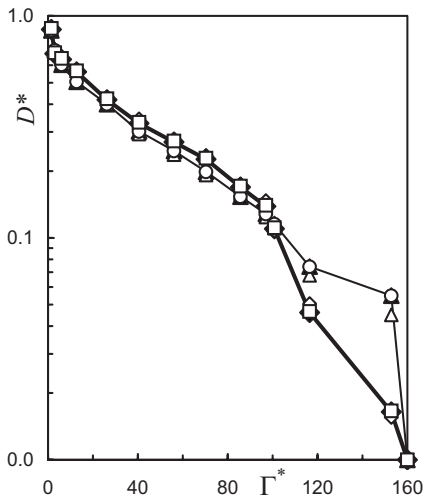

FIG. 6. D^* vs Γ^* for various potentials U: black symbols $U/U_c=\exp(-4r/l_p)+0.05l_p/r$; white symbols ; for different ξ: ($\diamond$, $\blacklozenge$) 1.86, $\square$ 0.93, $\bigcirc$ 0.23, and ($\triangle$, $\blacktriangle$) 0.12. The solid lines are the averaged data of simulation for quasi-2D systems with ξ <0.25 (thick line) and $\xi>0.3$ (fine line).

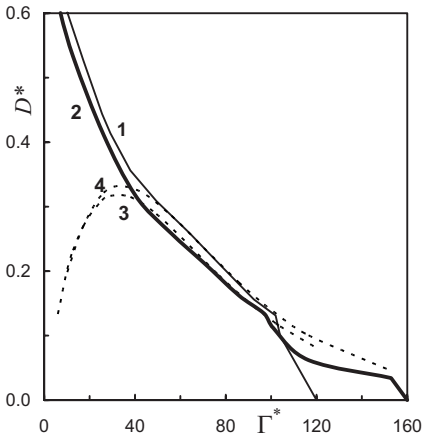

FIG. 7. D^* vs Γ^* for (1) 3D systems (see Ref. [13]); (2) quasi-2D systems (averaged); (3) Eq. (23) for 2D case with Γ_c^* =98; (4) Eq. (23) for 3D problem with Γ_c^*=102.

the diffusion coefficients is shown in Fig. 7. The accuracy of this approximation, which for $\Gamma^*>50$ is just within 5%, decreases to within 35% with decreasing parameter Γ^* down to the value of $\Gamma^*\approx 30$ [14–16]. It should be noted that the relation (23) is in accordance with the empirical "jump" theory developed for molecular fluids that is based on analogies between the liquid and the solid states of matter [1,4]; and it allows experimental determination of Γ^* in a strongly coupled system from measurements of the mean interparticle distance l_p, temperature T_p, and diffusion coefficient D without additional physical assumptions on the character of the pair potential [18].

The comparison of the evolution of mass-transfer processes in liquidlike 3D and quasi-2D systems with the behavior of the analytical $D_{MSD}(t)$, $\langle V_x(0)V_x(t)\rangle$, and $D_{GK}(t)$ functions, obtained for the harmonic oscillator, Eqs. (9), (13), and (14), demonstrates a good agreement for observation times $\nu_{fr}t \leq 1/\xi$ (see Figs. 2, 3, and 5). Thus, in accordance with the jump theory mentioned, the time of activation τ_0 of jumps (the mean time of settled life of the particles) in the simulated systems hardly depends on temperature and is defined by the oscillation frequency of the grains in the settled condition: $\tau_0 \approx 2/\omega_c$. The simulations also show that the system of interacting particles can be characterized by constant values of the transport coefficients only for intervals $t \gg \tau_0$, in contrast to the system of Brownian particles, for which the evolution function $D_{MSD}(t)$ [or $D_{GK}(t)$] tends to D_0 for $t \gg \nu_{fr}^{-1}$.

Measurement of the functions $\langle V(0)V(t)\rangle$, $D_{MSD}(t)$, and $D_{GK}(t)$ at short observation times can be useful for the passive diagnostics of dust components in nonideal plasmas in the case of local statistical equilibrium of a dusty subsystem. As all the mentioned functions are connected by the relationships (15a) and (15b) and unambiguously depend on such parameters of the grains as their temperature T, characteristic frequency ω_c, and the friction coefficient ν_{fr}, it is possible to simultaneously determine all the mentioned parameters by measuring any one of the functions $\langle V(0)V(t)\rangle$, $D_{MSD}(t)$, or $D_{GK}(t)$ and using a procedure of best fitting of this chosen function by the corresponding analytical function for the harmonic oscillator. Additionally, the information on T and ω_c

allows one to estimate the value of the coupling parameter Γ^* of the system under study from Eqs. (21) and (22).

V. CONCLUSIONS

The results of numerical investigation of mass-transfer processes in extensive quasi-two-dimensional and three-dimensional nonideal dissipative systems are presented. The particles in these systems interacted via various isotropic pair potentials, which represented different combinations of power-law and exponential functions, commonly used for simulation of repulsion in kinetics of interacting particles. The calculations were performed in a wide range of parameters typical for laboratory dusty plasmas in gas discharges.

The evolution of mass-transfer processes, the velocity autocorrelation functions, and the diffusion constants were studied. It was found that for the systems under study the particle temperature, the effective coupling parameter, and the scaling parameter determine all mentioned characteristics. It was shown that the evolution of the mean-square displacement of particles for short observation times corresponds to lattice oscillations with frequency proportional to the second derivative of the pair potential of interparticle interaction. Estimations of the characteristic oscillation frequencies of particles (ω_c) in 3D bcc structures and in 2D hexagonal lattices are presented. It is shown that these frequencies are responsible for the time of settled life of particles ($\tau_0 \approx 2/\omega_c$) in nonideal liquid systems and define the behavior of mass-transfer processes at short observation times ($t < \tau_0$). The obtained results are in good agreement with the jump theory.

The presented results can be used for the passive diagnostics of dusty component parameters in plasmas, as well as for the investigation of fast processes for physically short times insufficient for the description of these processes using the equations of macroscopic kinetics.

ACKNOWLEDGMENTS

This work was partially supported by the Russian Foundation for Fundamental Research (Project No. 07-08-00290), by the Program of the Presidium of RAS, and by the Russian Science Support Foundation.

[1] Ya. I. Frenkel, *Kinetic Theory of Liquids* (Oxford University Press, Oxford, 1976).
[2] *Photon Correlation and Light Beating Spectroscopy*, edited by by H. Z. Cummins and E. R. Pike (Plenum, New York, 1974).
[3] R. Balescu, *Equilibrium and Nonequilibrium Statistical Mechanics* (Wiley Interscience, Chichester, U.K., 1975).
[4] N. H. March and M. P. Tosi, *Introduction to Liquid State Physics* (World Scientific, Singapore, 1995).
[5] A. A. Ovchinnikov, S. F. Timashev, and A. A. Belyy, *Kinetics of Diffusion Controlled Chemical Processes* (Nova Science, Commack, NY, 1989).
[6] R. K. Dodd, J. C. Eilbeck, J. Gibbon, and H. C. Morris, *Solitons and Nonlinear Wave Equations* (Academic, New York, 1982).
[7] H. M. Thomas and G. E. Morfill, Nature (London) **379**, 806 (1996).
[8] V. E. Fortov, A. P. Nefedov, O. F. Petrov, A. A. Samarian, and A. V. Chernyschev, Phys. Rev. E **54**, R2236 (1996).
[9] V. Fortov *et al.*, Phys. Lett. A **258**, 305 (1999).
[10] O. S. Vaulina, O. F. Petrov, and V. E. Fortov, JETP **99**, 711 (2005).
[11] O. S. Vaulina and I. E. Drangevski, Phys. Scr. **T73**, 577 (2006).
[12] O. S. Vaulina and S. V. Vladimirov, Phys. Plasmas **9**, 835 (2002).
[13] O. S. Vaulina, S. V. Vladimirov, O. F. Petrov, and V. E. Fortov, Phys. Plasmas **11**, 3234 (2004).
[14] U. Konopka, L. Ratke, and H. M. Thomas, Phys. Rev. Lett. **79**, 1269 (1997).
[15] J. E. Daugherty, R. K. Porteous, M. D. Kilgore, and D. B. Graves, J. Appl. Phys. **72**, 3934 (1992).
[16] J. E. Allen, Phys. Scr. **45**, 497 (1992).
[17] D. Montgomery, G. Joyce, and R. Sugihara, Plasma Phys. **10**, 681 (1968).
[18] O. S. Vaulina *et al.*, Plasma Phys. Rep. **29**, 642 (2003).
[19] H. Totsuji *et al.*, Phys. Lett. A **221**, 215 (1996).
[20] O. S. Vaulina, K. G. Adamovich, and I. E. Dranzhevski, Plasma Phys. Rep. **31**, 562 (2005).